AAPS PharmSciTech, Vol. 13, No. 4, December 2012 (© 2012)
DOI: 10.1208/s12249-012-9842-z

Research Article

Enhanced Dissolution and Stability of Lansoprazole by Cyclodextrin Inclusion Complexation: Preparation, Characterization, and Molecular Modeling

Yi Lu,[1] Tao Guo,[2] Jianping Qi,[1] Jiwen Zhang,[2,3,4] and Wei Wu[1,4]

Received 19 May 2012; accepted 15 August 2012; published online 12 September 2012

Abstract. In this study, lansoprazole (LSP)/cyclodextrin (CD) inclusion complexes were prepared using a fluid bed coating technique, with β-cyclodextrin (β-CD) and 2-hydroxypropyl-β-cyclodextrin (HPCD) as the host molecules, respectively, to simultaneously improve the dissolution and stability of LSP. The dissolution rate and stability of LSP was dramatically enhanced by inclusion complexation regardless of CD type. LSP/HPCD inclusion complex was more stable under illumination than LSP/β-CD inclusion complex. Differential scanning calorimetry and powder X-ray diffractometry proved the absence of crystallinity in both LSP/CD inclusion complexes. Fourier transform infrared spectroscopy together with molecular modeling indicated that the benzimidazole of LSP was included in the cavity of both CDs, while LSP was more deeply included in HPCD than β-CD. The enhanced photostability was due to the inclusion of the sulfinyl moiety into the HPCD cavity. CD inclusion complexation could improve the dissolution and stability of LSP.

KEY WORDS: cyclodextrin; dissolution; inclusion complex; lansoprazole; molecular modeling; stability.

INTRODUCTION

Lansoprazole (LSP) is a substituted benzimidazole (Fig. 1) and selectively inhibits the H^+/K^+-ATPase of the parietal cell of the stomach (1). As a representative proton pump inhibitor, LSP has been clinically used in the therapy of gastric and duodenal ulcerative disease with a superior or equivalent clinical efficacy to H_2 receptor antagonist (2,3). However, the bioavailability of LSP was not consistent with wide intersubject variation (1,4), which is ascribed to the variation in the genotype of CYP2C19, possible degradation by the gastric acid, and limited water solubility (4–6). Besides, LSP, as presented in formulations, suffer from chemical degradation due to its sensitivity to low pH and light (7). Solid dispersions of LSP/polyvinylpyrrolidone (PVP) system prepared by the fluid-bed coating techniques (8), as well as mixtures of LSP and surfactants adsorbed to porous particles (6), have been employed to improve the dissolution and oral bioavailability of LSP. Although alkalizers can be used in LSP formulations as stabilizers and dissolution enhancers, they may affect the physiocochemical properties of the drugs (9). It is of importance to develop new LSP formulations that can provide both enhanced dissolution and stability.

The potential use of cyclodextrins (CDs) for the improvement of the solubility, stability, and/or bioavailability by inclusion complexation with drugs has been extensively studied (10,11). CDs are cyclic organic compounds composed of (α-1,4)-linked α-D-glucopyranose units. Due to the chair configuration of the glucopyranose units, the hydroxyl groups are oriented to the exterior of the CDs ring while the skeletal carbon and ethereal oxygen moieties of the glucose residue are lined to the center, which makes the entire CD molecule water soluble with a hydrophobic cavity to host a variety of hydrophobic guest molecules. This peculiar structure has been the basis of many pharmaceutical applications of inclusion complexes (12,13). The hypothesis of this study is that inclusion of LSP into CD cavity improves its dissolution and enhances its stability by encapsulating the labile moieties of LSP.

Among the cyclodextrin family, β-cyclodextrin (β-CD), containing seven (α-1,4)-linked α-D-glucopyranose units, is the most popular one due to its appropriate cavity size. However, the relatively strong binding of the cyclodextrin molecules in the crystal state make the aqueous solubility of β-CD much lower than its linear dextrin counterparts. In addition, β-CD molecules form intramolecular hydrogen bonds that diminish their ability to form hydrogen bonds with the surrounding water molecules (14). Derivation by alkylation of the free hydroxyl groups of the CDs can significantly increase water solubility. The ability of CDs to form inclusion complexes may also be enhanced by substitution on the hydroxyl groups (15–17). For years, modified CDs such as the highly water-soluble methylated and hydroxypropylated β-CDs have been used as solubilizing agents industrially. However, the differences in CDs' structure may result in different inclusion modes (17). It is important to compare LSP inclusion

[1] School of Pharmacy, Key Laboratory of Smart Drug Delivery of Ministry of Education and PLA, Fudan University, Shanghai 201203, China.
[2] Center for Drug Delivery Systems, Shanghai Institute of Materia Medica, State Key Laboratory of Drug Research, Chinese Academy of Sciences, Shanghai 201203, China.
[3] State Key Laboratory of Natural and Biomimetic Drugs, Peking University, Beijing 100191, China.
[4] To whom correspondence should be addressed. (e-mail: jwzhang@mail.shcnc.ac.cn; wuwei@shmu.edu.cn)

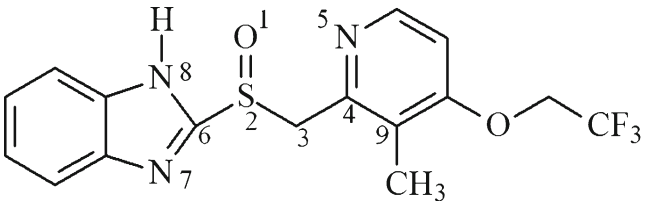

Fig. 1. Chemical structure of lansoprazole

complexes with β-CD and its hydroxypropylated derivative such as 2-hydroxypropyl-β-cyclodextrin (HPCD).

In this study, the inclusion complex of LSP with CDs (β-CD or HPCD) was prepared by a previously established fluid-bed coating method (8,18–20). The resultant inclusion complexes were characterized by dissolution study, differential scanning calorimetry (DSC), powder X-ray diffractometry, and Fourier transform-infrared spectrometry (FTIR) to verify the formation of inclusion complexes. It is assumed that improved dissolution and stability depend highly on the inclusion of the appropriate moieties. However, the conventional characterization tools can only provide ambiguous evidence on the molecular inclusion mechanisms. In the last decade, a large variety of computer-aided simulation techniques have been used to study the structural and energetic properties of CDs (21,22) and CD inclusion complexes (23–27), providing a general insight over a number of aspects of such systems. Therefore, the molecular mechanisms of inclusion were studied by molecular modeling to find evidence to support the improved dissolution and stability of LSP.

MATERIAL AND METHODS

Materials

LSP was purchased from Avilive pharmaceuticals (Zhejiang, China). β-CD (Yingmei®) was purchased from Yongguang Cyclodextrin Co. Ltd (Guangdong, China). HPCD (CAVASOL® W7 HP) with molar substitution (MS) of 0.9 was purchased from Maxdragon Biochemical Technology Co. Ltd (Guangzhou, China). PVP (Plasdone® K29/32) was a kind gift from China Division, ISP Chemicals Co. (Shanghai, China). Nonpareil pellets (Suglets® sugar spheres PF101, 710–850 μm in diameter) were provided by NP Pharm (Bazainville, France). Chromatographic methanol was a TEDIA product (USA). Deionized water was prepared by a Milli-Q water purifying system (Millipore, USA). All other reagents were of analytical grade.

Preparation of Inclusion Complex Pellets

LSP/CDs inclusion complex pellets were prepared in a Mini-Glatt fluid-bed coater (Wurster insert, Glatt GmbH, Binzen, Germany) following previously developed methods (8,18–20). Since LSP forms A_L-type inclusion complex with both β-CD and HPCD (28), the molar ratio of LSP/CDs was kept at 1/1. Briefly, CD was first dissolved in hot water and kept at 40°C. LSP was dissolved in 60% ethanol solution (adjusted to pH11.0 with NaOH) under continuous stirring until complete dissolution. The LSP solution was added gradually to the CD solution with intensive agitation, after which the mixture was allowed to cool down to room temperature under stirring. PVP K30 was added to the resulting solution at a weight ratio of 1/3 to the total solid of LSP/CD. The final solution was then sprayed through a nozzle onto fluidized non-pareil cores. The detailed operating conditions were as follows: inlet air temperature, 38°C; product temperature, 30°C; air flow rate, 98 m^3/h; spray rate, 1.0 mL min^{-1}; atomizing air pressure, 1.4–1.5 bar; and spray nozzle diameter, 0.5 mm. After completion, the pellets were dried for 15 min further at 32°C. The inclusion complexes were prepared at stoichiometric LSP/CDs ratio of 1/1 with a coating weight gain of 100%.

To minimize the interference of non-pareil cores with the physical characterization, the LSP/CDs inclusion complex was also prepared by spraying into the drying chamber without non-pareil cores under the same coating conditions and collected at the bottom.

Determination of LSP by HPLC

LSP was determined by high-performance liquid chromatography (HPLC)/UV following USP monograph procedures. The Agilent 1100 series HPLC system (Agilent, USA) was composed of a quaternary pump, a degasser, an autosampler, a column heater, and a tunable ultraviolet detector. LSP was separated by a C18 column (Diamonsil, 5 and 4.6×250 mm; Dikma, China) guarded with a refillable precolumn (C18, 2.0×20 mm, Alltech, USA) at 25°C and detected at 285 nm. The mobile phase was composed of a mixture of water, acetonitrile, and triethylamine (60:40:1, adjusted by phosphoric acid to a pH of 7.0) and pumped at a flow rate of 1.0 mL/min.

Dissolution Studies

The dissolution studies were performed using a ZRS-8G dissolution tester (Tianjin, China) based on Chinese Pharmacopoeia (ChP) method I (the rotating basket method). The samples, containing 10 mg of LSP, were sealed in hard gelatin capsules, then put into the rotating basket and immersed in 900 mL of phosphate buffer (pH7.4) thermostatically maintained at 37±0.5°C at a rotation speed of 100 rpm. At appropriate time intervals, 5 mL of the sample was withdrawn and filtered (Millex® AP, Millipore, 0.4 μm). The filtrate was analyzed by HPLC for LSP as described above. Meantime, preheated medium was added to keep a constant volume.

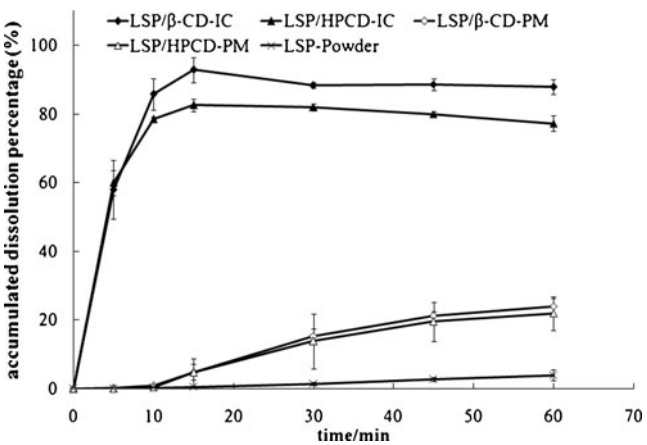

Fig. 2. Dissolution profiles of lansoprazole (LSP), LSP/β-CD physical mixture (LSP/β-CD-PM) and inclusion complexes (LSP/β-CD-IC), LSP/HPCD physical mixture (LSP/HPCD-PM) and inclusion complexes (LSP/HPCD-IC)

Differential Scanning Calorimetry

Thermal analysis of the samples (LSP, CDs, physical mixture, and inclusion complex powder) were carried out with a DSC 204A/G phoenix® instrument (Netzsch, Germany). About 10 mg of the sample was weighed into a nonhermetically sealed aluminum pan. The samples were heated from 40°C to 300°C at a heating rate of 10°C/min. The instrument was calibrated by using indium. All the DSC measurements were made in nitrogen atmosphere and the flow rate was 100 mL/min.

Powder X-ray Diffractometry

Powder X-ray Diffractometry (PXRD) of the samples (LSP, CDs, physical mixture, and inclusion complex powder) was performed with an X¢pert PRO X-ray diffractometer (Panalytical, Holland) over the 5.0–50° 2θ range at a scan rate of 4°/min, where the tube anode was Cu with Ka=0.154 nm monochromatized with a graphite crystal. Data was collected with 40 kV of tube voltage and 40 mA of tube current in step scan mode (step size, 0.02; counting time, 1 s/step).

Fourier Transform-Infrared Spectrometry

FTIR spectra of the samples (LSP, CDs, physical mixture, and inclusion complex powder) were obtained on a Nicolet Avatar 360 spectrometer (USA). The samples were first ground and mixed thoroughly with KBr, an infrared transparent matrix. The KBr disks were prepared by compressing the powder. The scans were obtained from 4,000 to 400 cm^{-1} at resolution of 1 cm^{-1}.

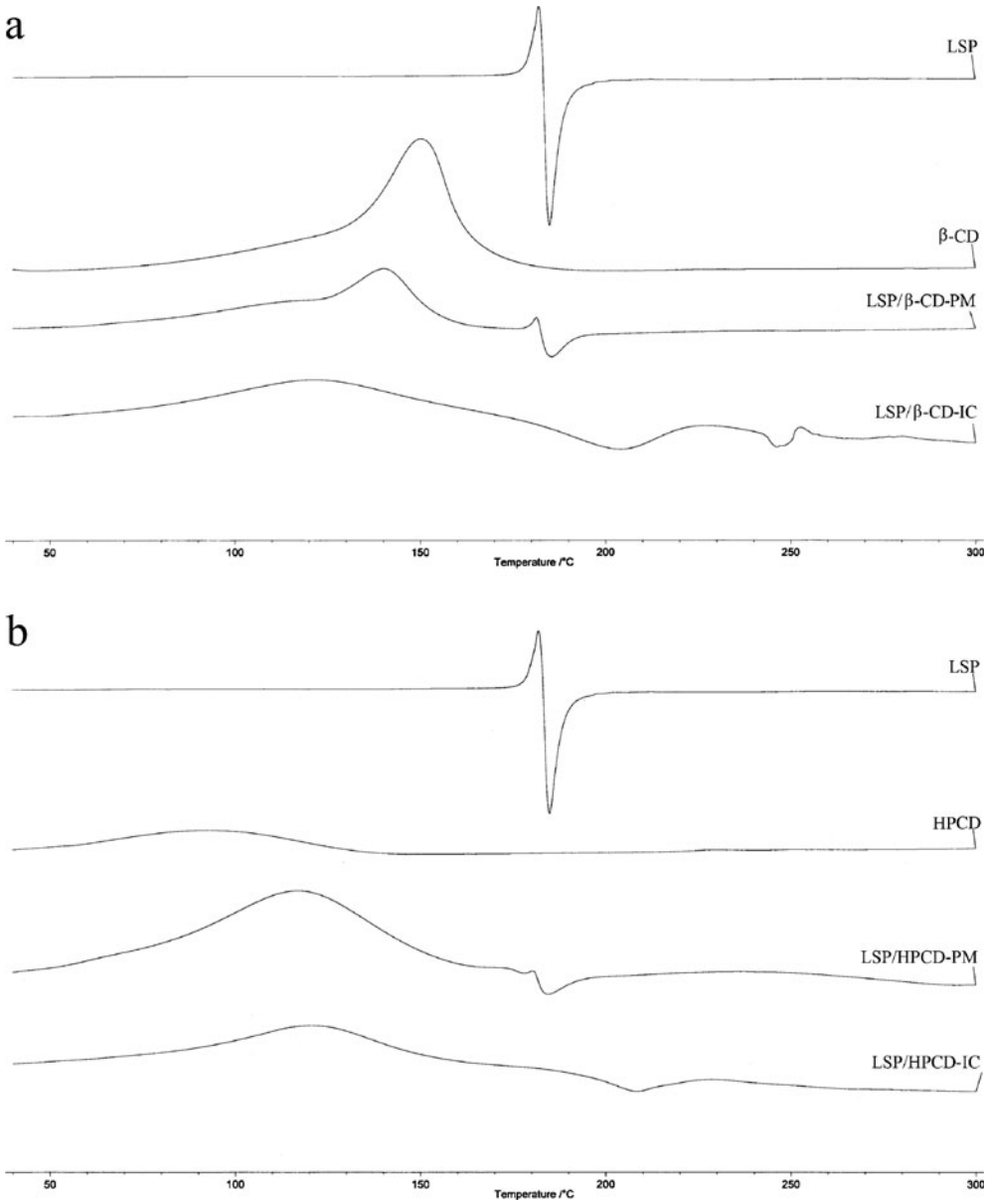

Fig. 3. **a** DSC thermogram of lansoprazole (LSP), β-CD, LSP/β-CD physical mixture (LSP/β-CD-PM) and inclusion complexes (LSP/β-CD-IC). **b** DSC thermogram of lansoprazole (LSP), HPCD, LSP/HPCD physical mixture (LSP/HPCD-PM) and inclusion complexes (LSP/HPCD-IC)

Stability Investigation

The influence of inclusion on stability of LSP against temperature, humidity, and photolysis was investigated according to the ChP stability testing guidelines. The temperatures tested were selected as 60°C and 40°C, respectively; humidity conditions were obtained in desiccators containing saturated solutions of inorganic salts: sodium chloride (75% RH) and potassium nitrate (92.5% RH); and the illumination intensity was set at 4,500±500 lx. Samples were put into flat weighing bottles and subjected to stress-testing conditions. After 5 days, samples equivalent to 10 mg LSP was weighed and extracted with 100 ml methanol for content determination by HPLC as described above. The concentration was defined as the percentage of the residue to the original concentration. The weight gain after 5 days in humidity conditions was also recorded and divided by the initial weight of the sample to get the moisture absorption.

Modeling and Methodology

The structure of β-CD was taken from crystal structures (PDB code: 1Z0N), while HPCD was constructed by adding 6 hydroxypropyl groups to 2-C of β-CD (MS 0.9; 29). The structure of LSP was constructed with Materials Studio 4.2 software. The Forcite program module in Materials Studio software was employed to implement the model calculations in this study and all patterns were optimized under the following standards: the total energy of the system $<2\times10^{-5}$ kcal mol^{-1}, the residual force <0.001 kcal/mol/Å and the displacement of atoms $<1\times10^{-5}$ Å. The COMPASS force field was employed to the molecular mechanics and molecular dynamics simulation and performed at 300 K for 100 fs with time step of 1 fs.

Complexation Process

The complexation process was performed as previously described methods (30). In brief, the origin of the Cartesian coordinate system was placed at the center of mass of the oxygens of the primary and secondary hydroxyl groups of the CD molecule. The *y*-axis passes through the centroids of both sides of the CD torus. The benzimidine or pyridine part of LSP approached by small steps the wider or narrower edge of the CD torus along the *y*-axis, respectively. The structures generated at each step are then optimized, allowing them to change from the initial conformations.

RESULTS AND DISCUSSION

Enhanced Dissolution

Dissolution of the inclusion complex pellets was studied at pH7.4 in phosphate buffer. Since the aqueous solubility of LSP at 25°C was determined to be 0.2187 mg/mL in preliminary studies (28), a volume of 900 ml dissolution medium was considered sufficient to provide a sink condition for the dissolution of as much as 10 mg of LSP.

As a water-insoluble drug, the dissolution of LSP powder was limited with a total of less than 5% dissolution at 60 min (Fig. 2). An enhanced dissolution of about 20% at 60 min was observed for both LSP/CDs physical mixtures, which was ascribed to the solubilization of the drug in aqueous CD solutions (18,31). The preparation of inclusion complex pellets, regardless of CD type, further increased the dissolution of LSP. The dissolution of LSP reached 80% at 15 min (Fig. 2). However, the dissolution profiles presented a slight decline tendency after 15 min. Inclusion is actually a dynamic process in the solution phase, free LSP molecules are in equilibrium with the molecules bound within the cyclodextrin cavity. Free LSP is susceptible to light and heat, the degradation of which will decrease the total amount of LSP in the dissolution medium.

Differential Scanning Calorimetry

DSC thermograms of LSP powder, LSP/CDs inclusion complex, and physical mixture are shown in Fig. 3a, b. The DSC thermogram of β-CD showed a broad endothermic effect, ranging from 70°C to 170°C (Fig. 3a), which may be attributable to the dehydration process (32). HPCD also showed a loss of water but at lower temperature around 100°C (Fig. 3b). LSP

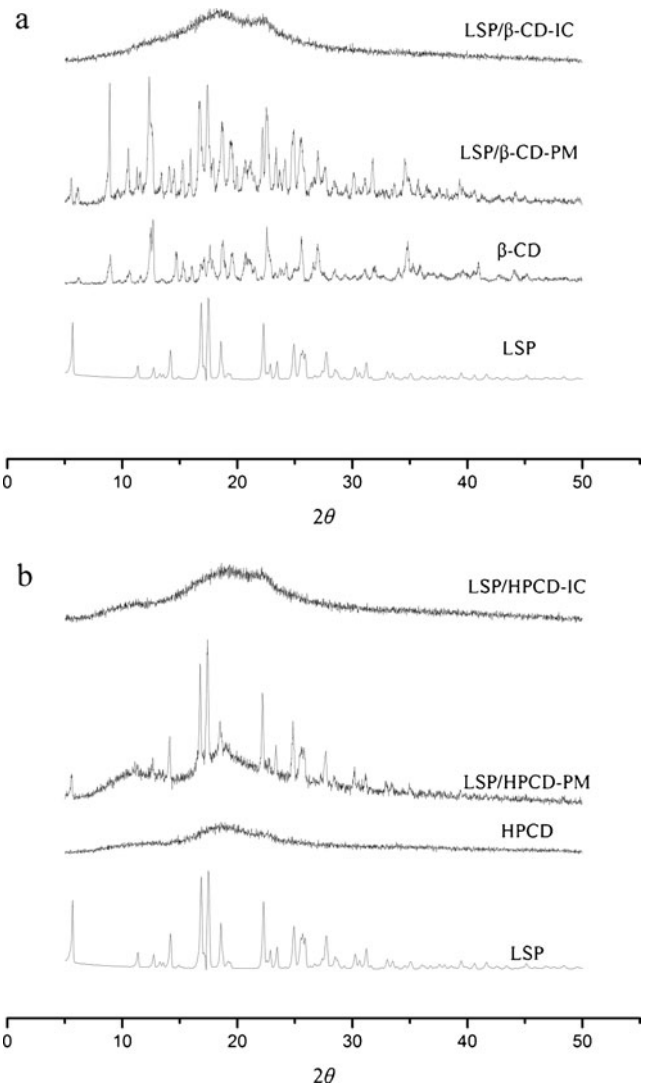

Fig. 4. **a** Powder X-ray diffractogram of lansoprazole (LSP), β-CD, LSP/β-CD physical mixture (LSP/β-CD-PM), and inclusion complexes (LSP/β-CD-IC). **b** Powder X-ray diffractogram of lansoprazole (LSP), HPCD, LSP/HPCD physical mixture (LSP/HPCD-PM), and inclusion complexes (LSP/HPCD-IC)

showed a sharp endothermic peak at 181.6°C corresponding to its melting point (Fig. 3). The thermogram of physical mixture, no matter which type of CD was used, was superimposable with their individual components. However, both the two binary systems prepared by the fluid-bed coating method showed the complete disappearance of the LSP endothermic peak, indicating the absence of crystallinity as a result of inclusion.

PXRD

LSP shows characteristic diffraction peaks at 11.331°, 14.160°, 16.835°, 17.458°, 18.584°, 22.262°, 24.906°, and 27.716° as shown in Fig. 4. β-CD showed a more complicated diffraction with peaks of almost equal intensity covering the range of 10–30° (Fig. 4a), while HPCD did not show distinct diffraction peaks (Fig. 4b). Similar to the results of DSC, the diffractograms of both physical mixture seemed like the superposition of each component. However, in the diffractograms of the inclusion complexes prepared by the fluid-bed coating technique, all of the diffraction peaks disappeared irrespective of CD or LSP (Fig. 4). This is typically for HPCD inclusion complex, as HPCD itself showed no distinct diffraction peaks and thus the inclusion of LSP into HPCD was similar to the formation of amorphous molecular dispersion. As far as the LSP/β-CD inclusion complex was concerned, the disappearance of LSP crystallinity may be attributable to the inclusion effect by β-CD, while the disappearance of the diffraction peaks of β-CD was ascribed to the dispersion effect of PVP K30 (18,19). However, since the total content of PVP K30 (about 25%) was much lower, the contribution of PVP K30 solid dispersion to enhance the dissolution of LSP was weak (18).

FTIR Spectroscopy

As seen from Fig. 5, the characteristic absorption peaks of LSP appeared at 1,580.2, 1,281.1, 1,117.8, and 1,037.7 cm^{-1}, respectively, denoting stretching vibration of C=N (νC=N) and C–N (νC–N) in benzimidazole, the ether band (ν–O–) and the sulfinyl (νS=O; Fig. 5; 8,33). In the physical mixture spectrum, the characteristic peaks of both LSP and CDs can be observed, and the spectrum can be regarded as a simple superposition of that of LSP and CDs (Fig. 5a, b).

However, obvious changes occurred in the feature and fingerprint region of the FTIR spectra of LSP/CD inclusion complex. As far as the peak at 1,580.2 cm^{-1} (νC=N) and 1,281.1 cm^{-1} (νC=N) was concerned, they shifted to higher wave number

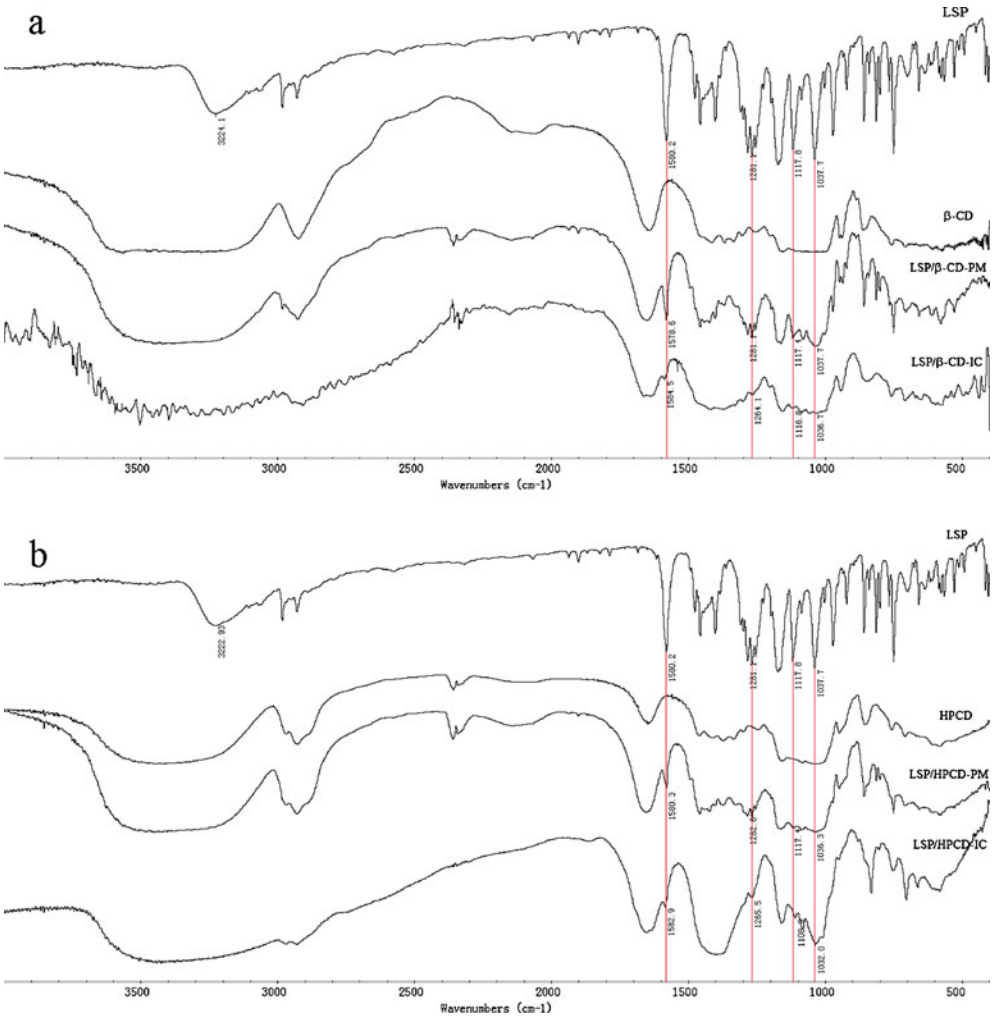

Fig. 5. **a** FTIR spectrogram of lansoprazole (LSP), β-CD, LSP/β-CD physical mixture (LSP/β-CD-PM), and inclusion complexes (LSP/β-CD-IC). **b** FTIR spectrogram of lansoprazole (LSP), HPCD, LSP/HPCD physical mixture (LSP/HPCD-PM), and inclusion complexes (LSP/HPCD-IC)

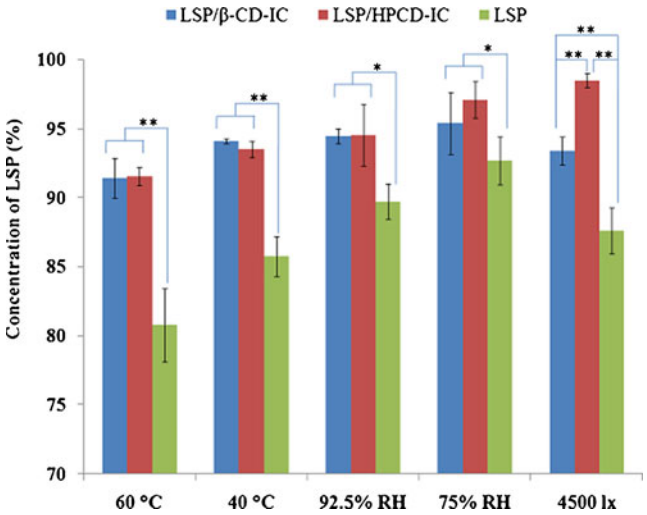

Fig. 6. Remained LSP concentration after 5-day investigation under high temperature (40°C and 60°C), high humidity (75% and 92.5% RH), and ilumination (4,500±500 lx) compared among LSP/β-CD inclusion complex, LSP/HPCD inclusion complex and free LSP (*P<0.05, **P<0.01)

bands and disappeared respectively in both β-CD and HPCD inclusion complexes. This is direct evidence indicating a possible inclusion of the benzimidazole ring into the CD cavities, which was similar to the inclusion pattern of omeprazole, an analog of LSP, in cyclodextrins (17). However, differences appeared when it came to the peak at 1,117.8 and 1,037.7 cm^{-1}. Both these two peak positions remained almost unchangeable for LSP/β-CD inclusion complex except for about 1 unit shift. These indicated that the ether and the sulfinyl moieties of LSP might be outside of the β-CD cavity. On the contrary, the shift of the ν–O– and νS=O by 5–10 cm^{-1} in the LSP/HPCD inclusion complex indicated that these groups were embedded in the HPCD cavity. It is easy to understand for the sulfinyl group since it is adjacent to the benzimidazole ring. The FTIR spectral disparity for this group might be ascribed to the inclusion depth as per different type of CDs. However, the ether band of LSP is away from the benzimidazole ring as shown in the structural formula (Fig. 1). It is possible for LSP to exist in a HPCD inclusion complex with a folded configuration, which needs to be identified by molecular modeling.

Stability

As reported previously (7), heat, humidity, and light all have significant impact on the stability of LSP. After 5 days, the concentration of LSP decreased in various degrees in different groups (Fig. 6). Heat showed the greatest impact on LSP stability as compared with other factors. The concentration of free LSP decreased to 80.78±2.64% and 85.76±1.42%, respectively at

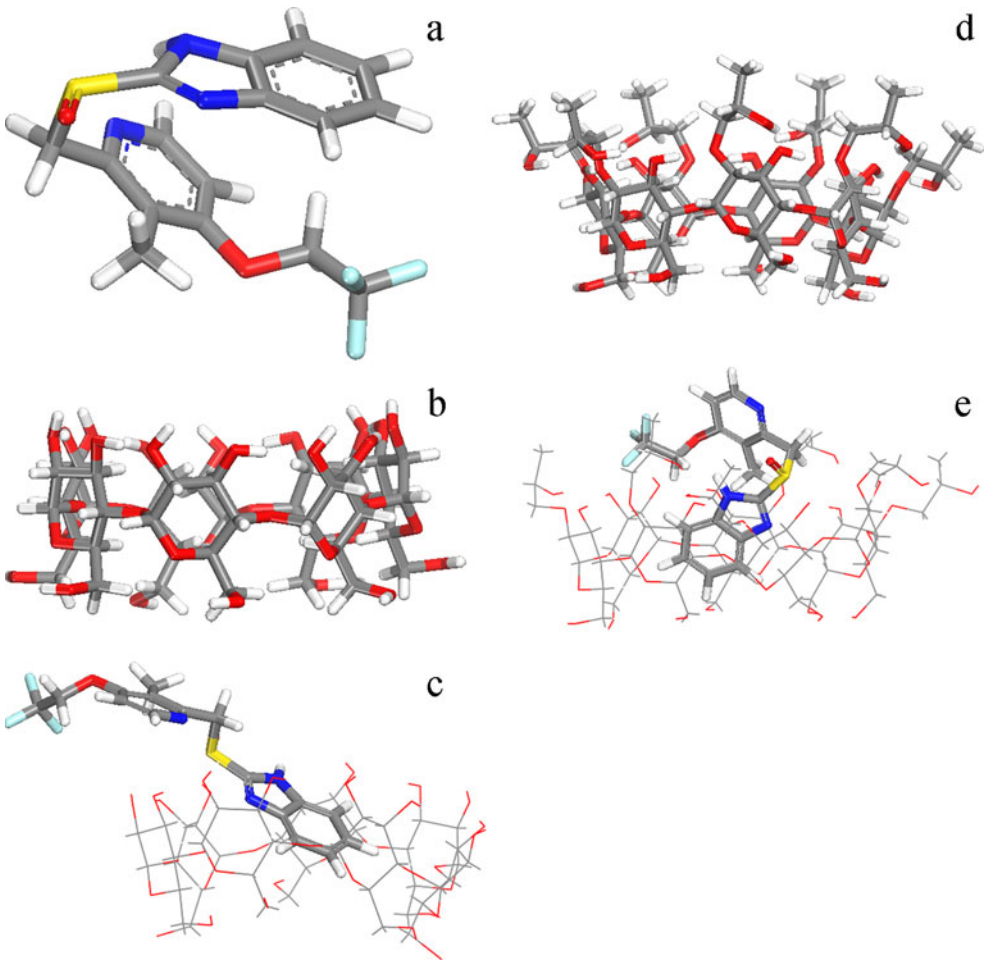

Fig. 7. Molecular model of LSP **a**, β-CD **b**, LSP/β-CD inclusion complex **c**, HPCD **d**, and LSP/HPCD inclusion complex **e**

60°C and 40°C after 5 days. The degradation of LSP under humid and irradiant conditions was about 10% after 5 days. However, regardless of the CD type, inclusion slowed down the degradation of LSP. The remained LSP concentrations in inclusion complexes were significantly higher than that of free drug in all tested conditions (Fig. 6), indicating good protective effects of CD. Moreover, both two types of CD showed similar stabilization effects to LSP under heat and humid test, since no significant differences were observed for the remaining LSP concentration. But interestingly, significant differences were presented in the photostability among different CD inclusions as well as free LSP with the order of LSP/HPCD inclusion complex>LSP/β-CD inclusion complex>LSP (Fig. 6).

The sulfinyl is the most fragile part of LSP, as it is common for this group to be reduced to sulfide or be ruptured when LSP is under degradation (7). Inclusion of the sulfinyl group into CD cavity and the consequent protective effects on this group is the determinative factor for LSP stability. As inferred from FTIR spectra, the sulfinyl group of LSP was included into the cavity of HPCD but not for β-CD, which was the main reason for the photostability disparity for these two inclusion complexes. However, at extreme temperatures of 60°C and 40°C, both two types of CD inclusion complexes showed similar stabilization effects on LSP. As far as high-humidity test was concerned, both HPCD and β-CD inclusion complex showed strong and comparative moisture absorption, which amounted to 15% and 5%, respectively, for 92.5% RH and 75% RH. A fraction of LSP/CD inclusion complex in the surface of the pellets may dissolve in the absorbed water causing free and included LSP to co-exist in dynamic equilibrium**.** The degradation of free LSP would break the equilibrium and prompt the release of free LSP from the inclusion complex, which will weaken the protective effects of CD. Therefore, there were no significant differences between HPCD and β-CD for stability improvement of LSP in humid conditions.

Although the stability of LSP was significantly enhanced by CD inclusion, it must be noticed that this is not the final dosage form due to the degradation of LSP in acidic media. An enteric layer needs to be coated outermost to avoid the degradation of LSP in upper gastrointestinal tract. In addition, LSP/CD inclusion complexes still got degraded in stress tests although with significantly enhanced stability. Due to highly sensitive to heat and light, a large quantity of alkaline stabilizers, occupying up to 10% (*w*/*w*) of LSP, is usually added to the LSP formulations to keep the stability, which, however, can affect the physicochemical properties of LSP (34). Incorporating of additional alkaline agents in the drug layer of the inclusion complex pellets will further increase the stability of the preparation, while the needed amount will be cut down due to the synergistic protective effects of CDs. These will be studied in the follow-up works. In this proof-of-concept study, the stability of the inclusion complexes is acceptable.

Molecular Modeling

The structure of LSP, CDs, and LSP/CD inclusion complexes are shown in Fig. 7. LSP presented a folding configuration (Fig. 7a), which is similar to the reported LSP conformation (35). The sulfoxide bond tends to remain in the same plane with the benzimidine ring, and the pyridine plane seems on a parallel with and superjacent to the benzimidine plane. After inclusion, the benzimidine of LSP was exclusively included into the wider aperture of cyclodextrin regardless of the CD type (Fig. 7c and e), which coincides well with the results of FTIR. However, the configuration of LSP was distorted through S2-C3-C4 to fill into the CD cavity. The greatest distortion was observed for LSP/β-CD inclusion complex as the pyridine plane revolved 180° around the S2-C3 axis and presented negative direction to the benzimidine plane (Fig. 7c). Consequently, the pyridine ring was located outside of the β-CD cylinder, and only a small part of benzimidine ring inserted into the cavity. The substitution of hydroxypropyl, in a sense, elongates the length of CD cylinder and broadens the opening of CD cavity (Fig. 7d). Then almost entire the LSP molecule, with minor changes of the initial conformation, was included into HPCD cavity. Since the sulfinyl and ether group of LSP are surrounded by hydroxypropyl of HPCD, the formation of hydrogen bond with hydroxyl will alter the infrared absorption of the corresponding groups, which elucidates the reason for the position shift of FTIR spectra of these two groups. In general, the results of molecular modeling coincided well with the inferences from FTIR investigation.

The results from molecular modeling also provide tangible evidence to support the presumption made for the photo stability. The sulfinyl of LSP was completely included inside of the hydroxypropyl cycle of HPCD (Fig. 7e), the shelter effects of hydroxypropyl explicitly account for the enhanced photostability by HPCD inclusion complex. With respect to LSP/β-CD inclusion complex, although the sulfinyl of LSP presented in the opening of β-CD, the OH-2 and OH-3 on the glucopyranose units might also have certain shelter effects on sulfinyl, which however was far weaker than that of hydroxypropyl in HPCD due to the smaller molecular volume. Thus, LSP/β-CD inclusion complex showed medium photostability.

CONCLUSIONS

Both LSP/β-CD and LSP/HPCD inclusion complex pellets were prepared by the fluid-bed coating technique. Significantly enhanced dissolution and stability of LSP was observed by both inclusion complexes. DSC and PXRD confirmed the formation of inclusion complexes. FTIR spectrometry together with molecular modeling indicated that the benzimidazole of LSP was included in the cavity of both CDs, while LSP was more deeply included in HPCD than β-CD. The HPCD inclusion complex showed stronger photostability than β-CD inclusion complex due to the deeper inclusion of LSP into the HPCD cavity.

ACKNOWLEDGMENTS

This study was supported by the Shanghai Commission of Education (10SG05) and the Shanghai Commission of Science and Technology (10430709200), the International Science and Technology Cooperation Project (S2010GR0920), and the Key National Science & Technology Projects (2010ZX09401-402).

REFERENCES

1. Gerloff J, Mignot A, Barth H, Heintze K. Pharmacokinetics and absolute bioavailability of lansoprazole. Eur J Clin Pharmacol. 1996;50:293–7.
2. Lew EA. Review article: pharmacokinetic concerns in the selection of anti-ulcer therapy. Aliment Pharmacol Ther. 1999;13 Suppl 5:11–6.

3. Stedman CA, Barclay ML. Review article: comparison of the pharmacokinetics, acid suppression and efficacy of proton pump inhibitors. Aliment Pharmacol Ther. 2000;14:963–78.
4. Sohn DR, Kwon JT, Kim HK, Ishizaki T. Metabolic disposition of lansoprazole in relation to the S-mephenytoin 4′-hydroxylation phenotype status. Clin Pharmacol Ther. 1997;61:574–82.
5. Pearce RE, Rodrigues AD, Goldstein JA, Parkinson A. Identification of the human P450 enzymes involved in lansoprazole metabolism. J Pharmacol Exp Ther. 1996;277:805–16.
6. Ito Y, Arai H, Uchino K, Iwasaki K, Shibata N, Takada K. Effect of adsorbents on the absorption of lansoprazole with surfactant. Int J Pharm. 2005;289:69–77.
7. DellaGreca M, Iesce MR, Previtera L, Rubino M, Temussi F, Brigante M. Degradation of lansoprazole and omeprazole in the aquatic environment. Chemosphere. 2006;63:1087–93.
8. Zhang XW, Sun NY, Wu BJ, Lu Y, Guan TZ, Wu W. Physical characterization of lansoprazole/PVP solid dispersion prepared by fluid-bed coating technique. Powder Technol. 2008;182:480–5.
9. Stroyer A, McGinity JW, Leopold CS. Solid state interactions between the proton pump inhibitor omeprazole and various enteric coating polymers. J Pharm Sci. 2006;95:1342–53.
10. Davis ME, Brewster ME. Cyclodextrin-based pharmaceutics: past, present and future. Nat Rev Drug Discov. 2004;3:1023–35.
11. Del Valle EMM. Cyclodextrins and their uses: a review. Process Biochem. 2004;39:1033–46.
12. Loftsson T, Brewster ME. Pharmaceutical applications of cyclodextrins. 1. Drug solubilization and stabilization. J Pharm Sci. 1996;85:1017–25.
13. Brewster ME, Loftsson T. Cyclodextrins as pharmaceutical solubilizers. Adv Drug Deliv Rev. 2007;59:645–66.
14. Loftsson T, Duchene D. Cyclodextrins and their pharmaceutical applications. Int J Pharm. 2007;329:1–11.
15. Ventura CA, Giannone I, Paolino D, Pistara V, Corsaro A, Puglisi G. Preparation of celecoxib-dimethyl-β-cyclodextrin inclusion complex: characterization and *in vitro* permeation study. Eur J Med Chem. 2005;40:624–31.
16. Kang J, Kumar V, Yang D, Chowdhury PR, Hohl RJ. Cyclodextrin complexation: influence on the solubility, stability, and cytotoxicity of camptothecin, an antineoplastic agent. Eur J Pharm Sci. 2002;15:163–70.
17. Figueiras A, Sarraguca JM, Carvalho RA, Pais AA, Veiga FJ. Interaction of omeprazole with a methylated derivative of β-cyclodextrin: phase solubility, NMR spectroscopy and molecular simulation. Pharm Res. 2007;24:377–89.
18. Lu Y, Zhang XW, Lai J, Yin ZN, Wu W. Physical characterization of meloxicam-β-cyclodextrin inclusion complex pellets prepared by a fluid-bed coating method. Particuology. 2009;7:1–8.
19. Zhang XW, Wu DN, Lai J, Lu Y, Yin ZN, Wu W. Piroxicam/2-hydroxypropyl-β-cyclodextrin inclusion complex prepared by a new fluid-bed coating technique. J Pharm Sci. 2009;98:665–75.
20. Sun NY, Wei XL, Wu BJ, Chen J, Lu Y, Wu W. Enhanced dissolution of silymarin/polyvinylpyrrolidone solid dispersion pellets prepared by a one-step fluid-bed coating technique. Powder Technol. 2008;182:72–80.
21. Manunza B, Deiana S, Pintore M, Gessa C. Structure and internal motion of solvated β-cyclodextrine: a molecular dynamics study. J Mol Struct. 1997;419:133–7.
22. Starikov EB, Brasicke K, Knapp EW, Saenger W. Negative solubility coefficient of methylated cyclodextrins in water: a theoretical study. Chem Phys Lett. 2001;336:504–10.
23. Lawtrakul L, Viernstein H, Wolschann P. Molecular dynamics simulations of β-cyclodextrin in aqueous solution. Int J Pharm. 2003;256:33–41.
24. Jursic BS, Zdravkovski Z, French AD. Molecular modeling methodology of β-cyclodextrin inclusion complexes. J Mol Struct. 1996;366:113–7.
25. Alvira E, Mayoral JA, Garcia JI. Molecular modelling study of β-cyclodextrin inclusion complexes. Chem Phys Lett. 1997;271:178–84.
26. Faucci MT, Melani F, Mura P. Computer-aided molecular modeling techniques for predicting the stability of drug-cyclodextrin inclusion complexes in aqueous solutions. Chem Phys Lett. 2002;358:383–90.
27. Chen W, Chang CE, Gilson MK. Calculation of cyclodextrin binding affinities: energy, entropy, and implications for drug design. Biophys J. 2004;87:3035–49.
28. Lu Y, Tang N, Qi JP, Wu W. Phase solubility behavior of hydrophilic polymer/cyclodextrin/lansoprazole ternary system studied at high polymer concentration and by response surface methodology. Pharm Dev Technol. 2012;17:236–41.
29. Mura P, Bettinetti G, Melani F, Manderioli A. Interaction between naproxen and chemically modified β-cyclodextrins in the liquid and solid state. Eur J Pharm Sci. 1995;3:347–55.
30. Madrid JM, Villafruela M, Serrano R, Mendicuti F. Experimental thermodynamics and molecular mechanics calculations of inclusion complexes of 9-methyl anthracenoate and 1-methyl pyrenoate with β-cyclodextrin. J Phys Chem B. 1999;103:4847–53.
31. Ghorab MM, Abdel-Salam HM, El-Sayad MA, Mekhel MM. Tablet formulation containing meloxicam and β-cyclodextrin: mechanical characterization and bioavailability evaluation. AAPS PharmSciTech. 2004;5:e59.
32. Montassier P, Duchene D, Poelman MC. Inclusion complexes of tretinoin with cyclodextrins. Int J Pharm. 1997;153:199–209.
33. Das S, Malik S, Jain B, Saini S. Synthesis and physicochemical studies of copper complex of lansoprazole. Orient J Chem. 2009;25:1129–31.
34. He W, Yang M, Fan JH, Feng CX, Zhang SJ, Wang JX, *et al.* Influences of sodium carbonate on physicochemical properties of lansoprazole in designed multiple coating pellets. AAPS PharmSciTech. 2010;11:1287–93.
35. Riel MA, Kyle DE, Bhattacharjee AK, Milhous WK. Efficacy of proton pump inhibitor drugs against *Plasmodium falciparum in vitro* and their probable pharmacophores. Antimicrob Agents Chemother. 2002;46:2627–32.